Available online at www.sciencedirect.com
SCIENCE DIRECT
Journal of the European Ceramic Society 26 (2006) 111–115
www.elsevier.com/locate/jeurceramsoc

# Reaction sintering of lead zinc niobate–lead zirconate titanate ceramics

Seung-Ho Lee, Chang-Bun Yoon, Sung-Mi Lee, Hyoun-Ee Kim*

*School of Materials Science and Engineering, Seoul National University, Seoul 151-742, Republic of Korea*

Received 13 June 2004; received in revised form 5 October 2004; accepted 16 October 2004
Available online 8 December 2004

**Abstract**

Lead zinc niobate (PZN)–lead zirconate titanate (PZT) ceramics were produced by the reaction-sintering process. The specimens were prepared directly from a mixture of their constituent oxides without any calcination step. When 50% PZN was added to tetragonal $Pb(Zr_{0.47}Ti_{0.53})O_3$ ceramics, the densities and electrical properties were found to be optimal ($\rho = 7.91\ g/cm^3$, $K = 1947$ at 1 kHz and room temperature, $d_{33} = 530\ pC/N$, $k_p = 0.61$). However, the specimen containing more than 50% PZN showed reduced density and decreased electrical properties, due to the formation of pyrochlore phases. The improved densification behavior of the reaction-sintering process was attributed to the enhanced diffusion of lattice defects, which were created by differences in the ionic valence of the B-sites ions of the perovskite structure.


*Keywords:* PZT; PZN; Reaction sintering, Piezoelectric properties

## 1. Introduction

Lead zirconate titanate ($Pb(Zr,Ti)O_3$; PZT) ceramics have been regarded as one of the most important ferroelectrics due to their excellent dielectric, piezoelectric and electro-optic properties.[1–3] PZT-based solid solution systems have been investigated by incorporating them with other $ABO_3$-type perovskites, especially relaxor-type materials, for the purpose of improving their sinterability, and their dielectric and piezoelectric properties.[4–7]

Among the numerous relaxor-type perovskites with an $A(B'B'')O_3$ structure, lead zinc niobate ($Pb(Zn_{1/3}Nb_{2/3})O_3$; PZN) is a typical relaxor ferroelectric material with a broad phase transition region and large dielectric constants.[8–11] However, single phase PZN is difficult to sinter in the perovskite structure by the conventional ceramic process, due to the formation of the pyrochlore phase.[12] The addition of other perovskite materials, such as barium titanate ($BaTiO_3$),[13] lead titanate ($PbTiO_3$)[14] or PZT,[5] has been found to be effective in stabilizing PZN in the perovskite structure. Especially, when tetragonal PZT ($Pb(Zr_{0.47}Ti_{0.53})O_3$) was incorporated with PZN by a conventional solid-state reaction method, a stable perovskite phase with excellent piezoelectric properties was obtained.[5] However, all of these processes employed a calcination step for the purpose of phase formation, as well as a sintering step for densification.

Recently, there have been reports that relaxor-based ceramics were prepared by reaction sintering, where the oxide mixtures were directly sintered at high temperature without undergoing the calcination step.[15–17] Reaction sintering is a simple and economical processing technique, in which the reactions between the constituents take place during sintering at high temperatures. However, PZT-based ceramics were difficult to prepare by reaction sintering, because large amounts of excess PbO were needed to induce the liquid phase sintering.[18,19]

The purpose of this study is to investigate the sintering behavior and electrical properties of PZN–PZT ceramics prepared by the reaction-sintering process. Different amounts

* Corresponding author. Fax: +82 2 884 1413.
*E-mail address:* kimhe@snu.ac.kr (H.-E. Kim).

0955-2219/$ – see front matter © 2004 Elsevier Ltd. All rights reserved.
doi:10.1016/j.jeurceramsoc.2004.10.005

of PZN were added to tetragonal $Pb(Zr_{0.47}Ti_{0.53})O_3$ ceramics and then the densification behavior and microstructure evolution of the PZN–PZT ceramics were systematically observed. The phase evolution, dielectric properties and piezoelectric properties were measured and correlated with the composition and densification behavior of the system.

## 2. Experimental procedure

PZN–PZT ceramics with the nominal composition $Pb[(Zn_{1/3}Nb_{2/3})_x(Zr_{0.47}Ti_{0.53})_{1-x}]O_3$ $(0.2 \leq x \leq 0.8)$ were prepared by conventional solid state reactions. Commercial oxide powders of PbO, ZnO, $Nb_2O_5$, $TiO_2$ (99.9% purity, Aldrich Chemicals, USA) and $ZrO_2$ (99% purity, Aldrich Chemicals, USA) were used as the starting materials. Appropriate amounts of PbO, ZnO, $Nb_2O_5$, $ZrO_2$ and $TiO_2$ for the stoichiometric PZN–PZT were milled in alcohol with $ZrO_2$ balls for 4 h, following which the slurry was dried. The milled powders were directly pressed into 10 or 15 mm diameter pellets without calcination, and then isostatically pressed at 200 MPa.

The pressed pellets were sintered in air at 1200 °C for 2 h using sealed alumina crucibles. A lead atmosphere was employed to minimize the evaporation of PbO during sintering, by using an equimolar mixture of PbO and $ZrO_2$. An excess of 0.5 wt.% PbO was added to compensate for lead loss during sintering. The density of the sintered PZN–PZT pellets was measured by the water immersion method (Archimedes method). The sintered disks were lapped on their major faces and silver electrodes were made from a low-temperature silver paste by firing at 500 °C for 30 min to enable electrical measurements to be taken. The piezoelectric samples were poled in a silicone oil bath at 150 °C by applying an electric field of 2 kV/mm for 10 min and then cooling them under the influence of the electrical field. The samples were aged for 24 h prior to testing.

X-ray diffraction (XRD, MXP18A-HF, Cu Kα radiation, MAC Science, Tokyo, Japan) was used to determine the perovskite/pyrochlore phase ratio in the sintered specimens using the following equation:[20]

$$\%\,\text{Pyro} = \frac{(I_{222})_{\text{Pyro}}}{(I_{110})_{\text{Pero}} + (I_{222})_{\text{Pyro}}} \times 100 \quad (1)$$

The microstructure development was studied by means of a field-emission scanning electron microscope (FE-SEM, JSM-6330F, JEOL Technics, Tokyo, Japan). Dielectric measurements were taken at room temperature using an impedance analyzer (SI1260 Impedance/Gain-Phase Analyzer, Solartron, Berkshire, UK). The piezoelectric coefficient ($d_{33}$) was measured with a quasi-static piezoelectric $d_{33}$-meter (ZJ-3D, Institute of Acoustics Academic Sinica, Beijing, China). The electromechanical coupling factor ($k_p$) was measured by the resonance and anti-resonance technique using the impedance analyzer and was calculated from the following formula:

$$\frac{1}{k_p^2} = \frac{0.395 f_r}{f_a - f_r} + 0.574 \quad (2)$$

where $f_r$ and $f_a$ are the resonance and anti-resonance frequencies, respectively.[21] The field-induced longitudinal strain ($s_{33}$) was monitored by using a displacement sensor (DT/2/S, Solartron, West Sussex, UK) and a high voltage power supply source (BERTAN, Hicksville, NY, USA).

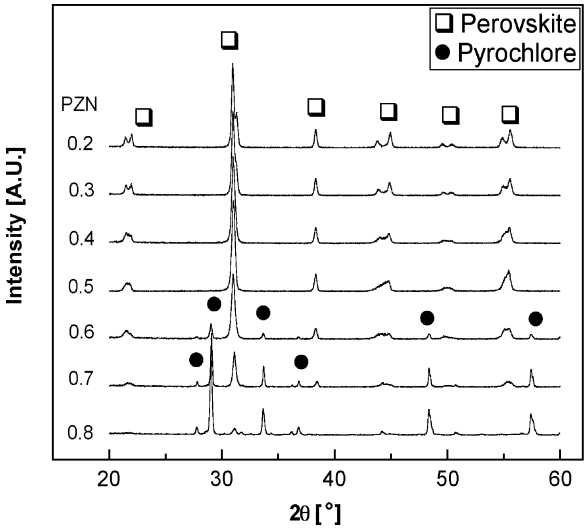


Fig. 1. X-ray diffraction patterns of $x$PZN − (1 − $x$)PZT (Zr/Ti = 47/53, $x$ = 0.2–0.8) specimens sintered at 1200 °C.

## 3. Results and discussion

The formation of the perovskite and pyrochlore phases in the $x$PZN − (1 − $x$)PZT (Zr/Ti = 47/53, $x$ = 0.2–0.8) specimens produced by the reaction-sintering process were studied and analyzed by XRD. The XRD patterns from this system are shown in Fig. 1. When 20% PZN was added, the tetragonal phase was formed in the specimen. As the PZN content increased to 30%, a weak rhombohedral peak began to appear. As the PZN content was further increased, the rhombohedral peak became stronger. Because PZN has a rhombohedral structure, the observation of increased rhombohedral peaks with increased PZN content was understandable. When the proportion of PZN added was 60%, pyrochlore phase began to form along with the perovskite phase. As the PZN content increased to 70% and 80%, the pyrochlore content was increased to 59% and 93%, respectively. These phase analyses indicated that the stable perovskite phase was formed in the PZN–PZT ceramics only when the PZN content was less than 60%.

Fig. 2A–C show the scanning electron microscopy images of the fracture surfaces of the $x$PZN − (1 − $x$)PZT

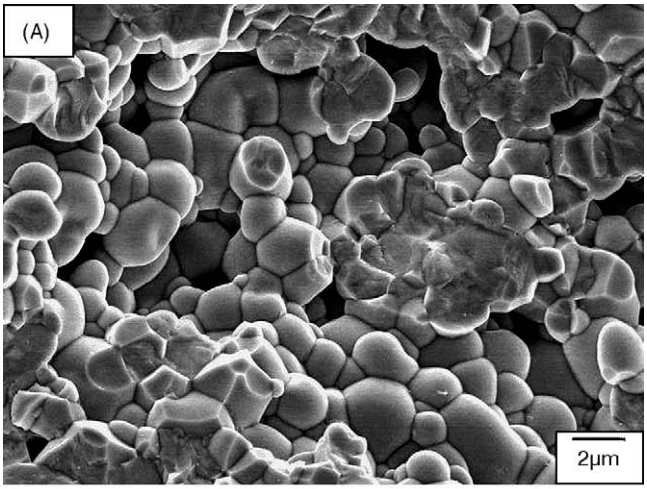


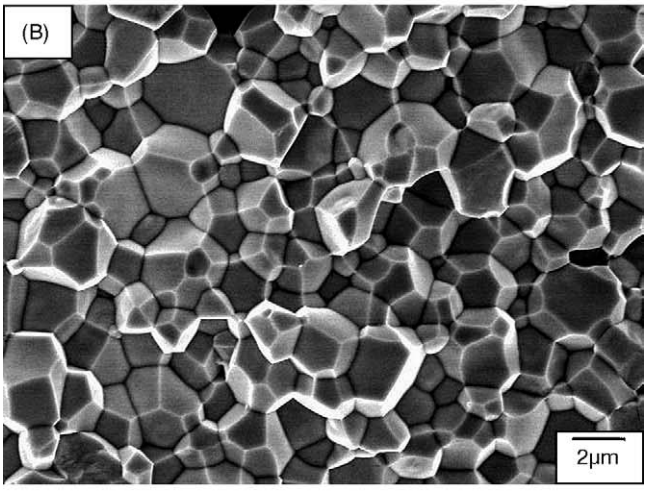


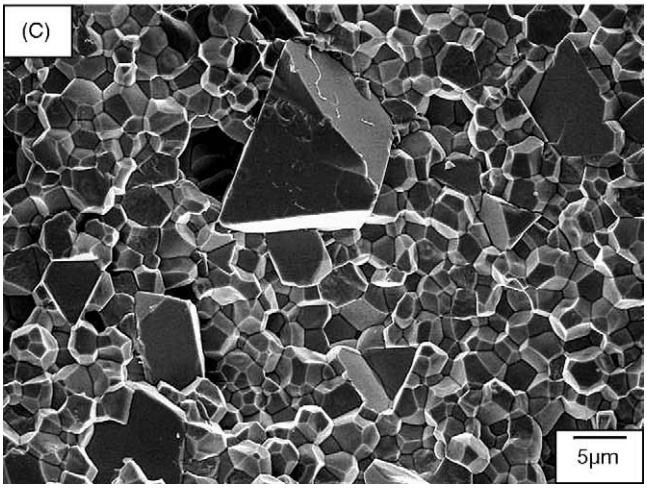


Fig. 2. SEM micrographs of the fracture surfaces of $x$PZN − (1 − $x$)PZT (Zr/Ti = 47/53) specimens sintered at 1200 °C: (A) $x$ = 0.2, (B) $x$ = 0.5, (C) $x$ = 0.6.

(Zr/Ti = 47/53, $x$ = 0.2, 0.5, 0.6) specimens produced by the reaction-sintering process. When 20% PZN was added to the specimen, a large number of pores were present, indicating insufficient densification of the specimen (Fig. 2A). As the PZN content increased, the specimens became more dense, so that when 50% PZN was added, the specimen was almost fully dense (Fig. 2B). With further addition of PZN, pyrochlore phases were formed, as shown in Fig. 2C. The formation of the pyrochlore phase was also observed by XRD analysis (Fig. 1).

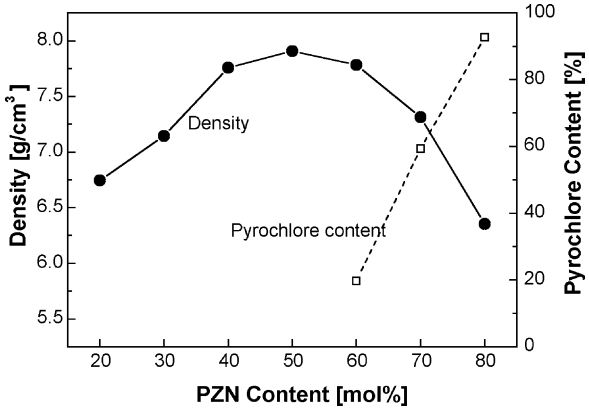


Fig. 3. Density and pyrochlore content of $x$PZN − (1 − $x$)PZT (Zr/Ti = 47/53, $x$ = 0.2–0.8) specimens sintered at 1200 °C.

The sintering behavior of PZN–PZT ceramics is highly correlated with the microstructure of the specimens. The density and pyrochlore content of the $x$PZN − (1 − $x$)PZT (Zr/Ti = 47/53, $x$ = 0.2–0.8) ceramics produced by the reaction-sintering process are shown in Fig. 3. The densification behavior of the specimen was greatly influenced by the PZN content. The specimen containing 20% PZN had a density of 6.75 g/cm$^3$ (82% of the theoretical density). As the PZN content was increased, the density increased steadily, as shown in Fig. 3. The highest density was obtained for this system when the PZN content was 50% ($\rho$ = 7.91 g/cm$^3$, 95% of the theoretical density). However, when the PZN content exceeded 50%, the density decreased rapidly, apparently due to the formation of pyrochlore phases. These results indicate that the addition of PZN to PZT enhances densification during the reaction-sintering process. However, too much PZN is detrimental to the densification process, because of the formation of pyrochlore phase.

The improvement in the sinterability of PZT brought about by the addition of PZN is believed to be closely related to the increased mobility of the ions. It is well known that lattice defects or vacancies are effective in promoting densification, because sintering is mainly controlled by the diffusion step.[22] These phenomena have been also observed in other systems. For example, the evaporation of PbO in PZT[22,25] or lead lanthanum zirconate titanate (PLZT)[23,24] generates oxygen and lead vacancies to a certain degree, thereby enhancing the transport of material and the process of densification that occur during the sintering process. In the present system, however, the evaporation of PbO was not one of the main factors, because it was identical for all the specimens. Instead, defects are deemed to have formed in the B-sites of the PZN–PZT perovskite structure, because the aliovalent ions

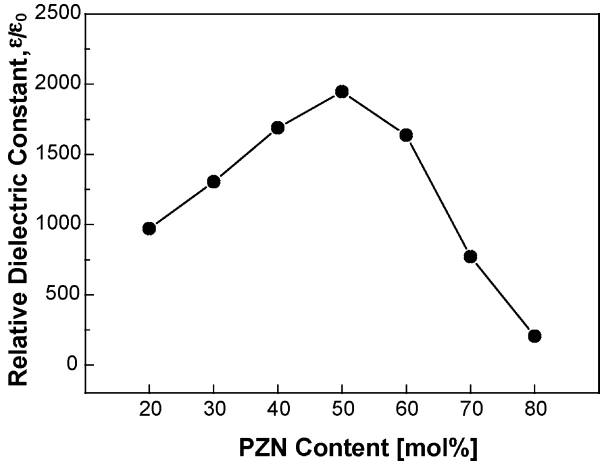


Fig. 4. Relative dielectric constant (measured at room temperature and 1 kHz) of $x$PZN – $(1-x)$PZT (Zr/Ti = 47/53, $x$ = 0.2–0.8) specimens sintered at 1200 °C as a function of the PZN content.

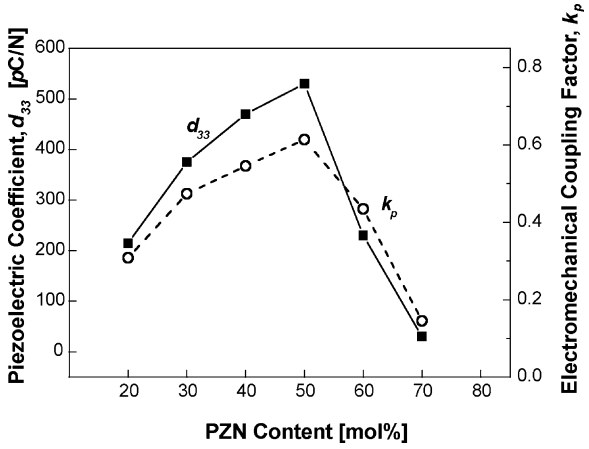


Fig. 5. Piezoelectric coefficients and electromechanical coupling factors of $x$PZN – $(1-x)$PZT (Zr/Ti = 47/53, $x$ = 0.2–0.8) specimens sintered at 1200 °C as a function of the PZN content.

($Zn^{2+}$, $Nb^{5+}$, $Zr^{4+}$, $Ti^{4+}$) in the B-sites can substitute for each other. When PZN was added to the PZT ceramics, portions of the $Zn^{2+}$ and $Nb^{5+}$ ions were substituted for the $Zr^{4+}$ and $Ti^{4+}$ ions, respectively, because the radius of $Zr^{4+}$ (0.082 nm) is almost equal to that of $Zn^{2+}$ (0.083 nm) and the radius of $Ti^{4+}$ (0.064 nm) is similar to that of $Nb^{5+}$ (0.069 nm).[26] In this case, the differences in ionic valence in the B-sites ions create a local charge imbalance as follows:

$$Zn^{2+} + 2Nb^{5+} \xrightarrow{Zr,Ti} Zn''_{Zr} + 2Nb_{Ti}^{\bullet} \quad (3)$$

Even though no vacancy was formed by this substitutional reaction, the mobility of the $Zn^{2+}$ and $Nb^{5+}$ ions is deemed to be much enhanced due to the charge imbalance. As the amount of PZN was increased, the concentration of these lattice defects ($Zn''_{Zr}$, $Nb_{Ti}^{\bullet}$) increased, thereby increasing the diffusion and densification rates in the sintering process. However, when the PZN content became higher than the PZT content, the concentration of lattice defects decreased because the amounts of the $Zr^{4+}$ and $Ti^{4+}$ ions substituting for the $Zn^{2+}$ and $Nb^{5+}$ ions decreased. Therefore, the specimen containing 50% PZN showed the highest density because the concentration of lattice defects reached the maximum value at this composition. In addition, when the PZN content exceeded 50%, secondary pyrochlore phases were formed, which affected the densification behavior adversely.

The electrical properties of the PZN–PZT ceramics exhibited a similar trend to the density profiles. The dielectric and piezoelectric properties increased when the PZN content in the specimens was increased. Fig. 4 shows the relative dielectric constant (measured at room temperature and 1 kHz) of the $x$PZN – $(1-x)$PZT (Zr/Ti = 47/53) ceramics. The piezoelectric coefficients ($d_{33}$) and electromechanical coupling factor ($k_p$) of the $x$PZN – $(1-x)$PZT (Zr/Ti = 47/53) ceramics are shown in Fig. 5. The poled specimens containing 80% PZN gave no piezoelectric response. Consequently, the $d_{33}$ and $k_p$ values of this composition are not available. When the PZN content was 20%, the electrical properties of the specimens were relatively low ($K$ = 971, $d_{33}$ = 215 pC/N, $k_p$ = 0.31). When more than 20% PZN was added, the electrical properties increased rapidly and reached a maximum value at 50% PZN ($K$ = 1947, $d_{33}$ = 530 pC/N, $k_p$ = 0.61). With further addition of PZN, the electrical properties decreased sharply because of the formation of pyrochlore phases and decrease in densities. The strain of the 0.5PZN–0.5PZT (Zr/Ti = 47/53) specimen produced by the reaction-sintering process is shown in Fig. 6. The coercive field for this specimen was 0.7 kV/mm and the strain at 2 kV/mm was about 0.26%, which was similar to that of the PZN–PZT specimens for which the calcination step was included in the fabrication process.[5]

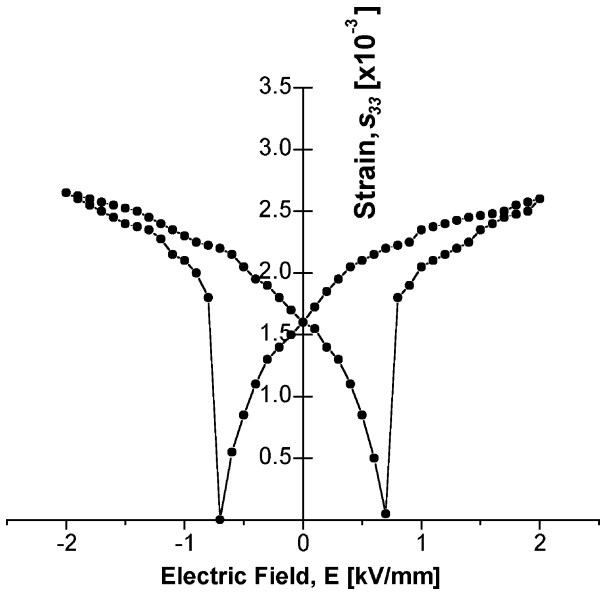


Fig. 6. Strain of 0.5PZN–0.5PZT (Zr/Ti = 47/53) specimen sintered at 1200 °C as a function of the electric field.

## 4. Conclusion

In this study, PZN–PZT ceramics were successfully prepared by the conventional solid-state ceramic process without the calcination step (reaction-sintering process). When 50% PZN was added to the tetragonal $Pb(Zr_{0.47}Ti_{0.53})O_3$ ceramics, followed by sintering in air at 1200 °C, the densities and electrical properties ($\rho = 7.91$ g/cm$^3$, $K = 1947$ at 1 kHz and room temperature, $d_{33} = 530$ pC/N, $k_p = 0.61$) were found to be optimal. However, when the PZN content exceeded 50%, the density and electrical properties began to decrease, due to the formation of pyrochlore phases. The densification behavior of the reaction-sintering process was greatly influenced by the enhanced diffusion of lattice defects, which were created as a result of differences in the ionic valence of the B-sites ions of the perovskite structure.

## References


1. Jaffe, B., Cook Jr., W. R. and Jaffe, H., *Piezoelectric Ceramics*. Academic Press, London, UK, 1971.
2. Xu, Y., *Ferroelectric Materials and Their Applications*. Elsevier Science, Amsterdam, The Netherlands, 1991.
3. Haertling, G. H., Ferroelectric ceramics: history and technology. *J. Am. Ceram. Soc.*, 1999, **82**, 797–818.
4. Moon, J. H. and Jang, H. M., Effects of sintering atmosphere on densification behavior and piezoelectric properties of $Pb(Ni_{1/3}Nb_{2/3})O_3$-$PbTiO_3$-$PbZrO_3$ ceramics. *J. Am. Ceram. Soc.*, 1993, **76**, 549–552.
5. Fan, H. Q. and Kim, H. E., Perovskite stabilization and electromechanical properties of polycrystalline lead zinc niobate-lead zirconate titanate. *J. Appl. Phys.*, 2002, **91**, 317–322.
6. Koval, V., Alemany, C., Briancin, J., Brunckova, H. and Saksl, K., Effect of PMN modification on structure and electrical response of $x$PMN-(1−$x$)PZT ceramic systems. *J. Eur. Ceram. Soc.*, 2003, **23**, 1157–1166.
7. Vittayakorn, N., Rujijanagul, G., Tunkasiri, T., Tan, X. and Cann, D. P., Perovskite phase formation and ferroelectric properties of the lead nickel niobate-lead zinc niobate-lead zirconate titanate ternary system. *J. Mater. Res.*, 2003, **18**, 2882–2889.
8. Yokomizo, Y., Takahashi, T. and Nomura, S., Ferroelectric properties of $Pb(Zn_{1/3}Nb_{2/3})O_3$. *J. Phys. Soc. Jpn.*, 1970, **28**, 1278–1284.
9. Kuwata, J., Uchino, K. and Nomura, S., Diffuse phase transitions in lead zinc niobate. *Ferroelectrics*, 1979, **22**, 863–867.
10. Kuwata, J., Uchino, K. and Nomura, S., Dielectric and piezoelectric properties of $0.91Pb(Zn_{1/3}Nb_{2/3})O_3$-$0.09PbTiO_3$ single crystals. *Jpn. J. Appl. Phys.*, 1982, **21**, 1298–1302.
11. Park, S. E. and Shrout, T. R., Ultrahigh strain and piezoelectric behavior in relaxor based ferroelectric single crystals. *J. Appl. Phys.*, 1997, **82**, 1804–1811.
12. Shrout, T. R. and Halliyal, A., Preparation of lead-based ferroelectric relaxors for capacitors. *Am. Ceram. Soc. Bull.*, 1987, **66**, 704–711.
13. Halliyal, A., Kumar, U., Newnham, R. E. and Cross, L. E., Stabilization of the perovskite phase and dielectric properties of ceramics in the $Pb(Zn_{1/3}Nb_{2/3})O_3$-$BaTiO_3$ system. *Am. Ceram. Soc. Bull.*, 1987, **66**, 671–676.
14. Gururaja, T. R., Safari, A. and Halliyal, A., Preparation of perovskite PZN-PT ceramic powder near the morphotropic phase boundary. *Am. Ceram. Soc. Bull.*, 1986, **65**, 1601–1603.
15. Chen, J. H., Liou, Y. C. and Tseng, K. H., Stoichiometric perovskite lead magnesium niobate ceramics produced by reaction-sintering process. *Jpn. J. Appl. Phys.*, 2003, **42**, 175–181.
16. Liou, Y. C., Stoichiometric perovskite PMN-PT ceramics produced by reaction-sintering process. *Mater. Sci. Eng.*, 2003, **B103**, 281–284.
17. Kong, L. B., Ma, J. and Zhang, R. F., Possibility of one-step approach to 0.7PZN-0.3BT multiple ceramics from component constituent oxides. *Mater. Lett.*, 2002, **53**, 205–210.
18. Kong, L. B. and Ma, J., PZT ceramics formed directly from oxides via reactive sintering. *Mater. Lett.*, 2001, **51**, 95–100.
19. Kong, L. B., Ma, J., Zhu, W. and Tan, O. K., Reaction sintering of partially reacted system for PZT ceramics via a high-energy ball milling. *Scripta Mater.*, 2001, **44**, 345–350.
20. Swartz, S. L. and Shrout, T. R., Fabrication of perovskite lead magnesium niobate. *Mater. Res. Bull.*, 1982, **17**, 1245–1250.
21. *IEEE Standard on Piezoelectricity*, *IEEE Standard 176-1978*. Institute of Electrical and Electronic Engineers, New York, 1978.
22. Atkin, R. B. and Fulrath, R. M., Point defects and sintering of lead zirconate-titanate. *J. Am. Ceram. Soc.*, 1971, **54**, 265–270.
23. Lin, W. K. and Chang, Y. H., Behavior of PbO in the two-stage sintering of PLZT ceramics. *Mater. Sci. Eng.*, 1994, **A186**, 177–183.
24. Choi, J. J., Ryu, J. and Kim, H. E., Microstructural evolution of transparent PLZT ceramics sintered in air and oxygen atmospheres. *J. Am. Ceram. Soc.*, 2001, **84**, 1465–1469.
25. Kingon, A. I. and Clark, J. B., Sintering of PZT ceramics: II. Effect of PbO content on densification kinetics. *J. Am. Ceram. Soc.*, 1983, **66**, 256–260.
26. Zhdanov, G. C., *Solid State Physics, Vol 1*. Moscow University Press, Moscow, 1961, p. 184.